A structured approach to forensic study of explosions: The TNO Inverse Explosion Analysis tool

M.M. van der Voort, R.M.M. van Wees, S.D. Brouwer, M.J. van der Jagt-Deutekom,

J. Verreault

TNO, Lange Kleiweg 137, 2280 AA Rijswijk, The Netherlands

martijn.vandervoort@tno.nl

Abstract

Forensic analysis of explosions consists of determining the point of origin, the explosive substance involved, and the charge mass. Within the EU FP7 project Hyperion, TNO developed the Inverse Explosion Analysis (TNO-IEA) tool to estimate the charge mass and point of origin based on observed damage around an explosion. In this paper inverse models are presented based on the two most frequently occurring and reliable sources of information: window breakage and building damage. The models have been verified by applying them to the Enschede firework disaster and the Khobar tower attack. Furthermore a statistical method has been developed to combine the various types of data, in order to determine an overall charge mass distribution.

In relatively open environments, like for the Enschede firework disaster, the models generate realistic charge masses that are consistent with values found in forensic literature. The confidence interval predicted by the IEA tool is however larger than presented in the literature for these specific cases. This is realistic due to the large inherent uncertainties in a generic tool. Furthermore, to our judgment often a too narrow range of charge masses is reported compared to the evidence. The IEA-models give a reasonable first order estimate of the charge mass in a densely built urban environment, such as for the Khobar tower attack. Due to blast shielding effects which are not taken into account in the IEA tool, this is usually an under prediction. To obtain more accurate predictions, the application of Computational Fluid Dynamics (CFD) simulations is advised.

The TNO IEA tool gives unique possibilities to inversely calculate the TNT equivalent charge mass based on a large variety of explosion effects and observations. The IEA tool enables forensic analysts, also those who are not experts on explosion effects, to perform an analysis with a largely reduced effort.

Keywords: explosion, forensic analysis, blast, debris, damage, statistical analysis

1. Introduction

Forensic analysis of explosions consists of determining the point of origin, the explosive substance involved, and the charge mass. In the case of deliberate explosions this information is desirable to trace production facilities of illicit materials and eventually the perpetrator. In the case of accidental explosions this information is important to identify the cause of the explosion, and to develop appropriate safety measures.

Although literature on post blast forensic investigation [1, 2, 3] contains a wealth of information, the descriptions are mainly qualitative. Furthermore the focus is on collecting explosive residues and possible remains of a bomb. The current paper presents a quantitative method to estimate the TNT equivalent charge mass and point of origin based on observed damage around the explosion. The

application of the method is limited to explosives which can be reasonably well represented by a TNT equivalency based on blast. This excludes e.g. gas or dust explosions.

The most frequently occurring and reliable sources of information are observations on window breakage and building damage [12, 13, 14, 15]. Also the size of a crater, fireball diameter, break- up of an enclosure in which the bomb was transported or placed and debris throw of the enclosure may provide valuable information. For the various phenomena we have developed inverse models, which give an estimate of the charge mass (including an error) typically as a function of damage level and distance. These models have been implemented in the TNO Inverse Explosion Analysis (IEA) tool, which was developed for on-site application by a forensic analyst [22, 23]. The tool enables the user to define evidence locations based on OpenStreetMaps, and add specific damage information. An example is given in Figure 1 for the entry of window breakage evidence.

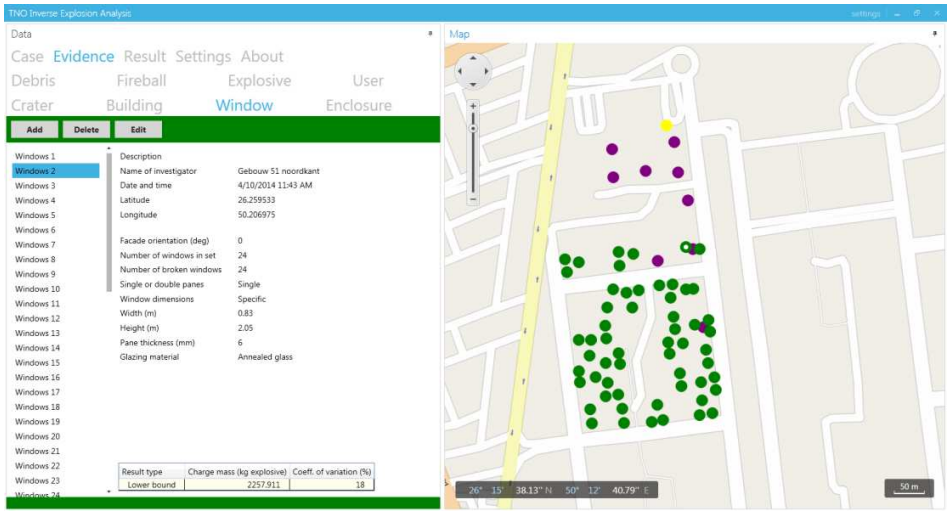

Figure. 1 Screenshot of the TNO IEA tool, Evidence tab with window evidence entry [22, 23].

Terrorist bombing attacks and accidental explosions are often humanitarian disasters. Although the number of fatalities and injured persons may exhibit a correlation with charge mass, we did not use this information for inverse calculations. The reason is the large inherent uncertainty in the location of persons during the explosion, their protection and vulnerability.

The inverse calculations lead to a set of charge mass estimates with varying reliability. Furthermore, some estimates give just a lower or upper bound. A statistical method has been developed to combine the various types of data, and to determine an overall charge mass distribution. This method is shortly described in Section 2.

In order to limit the scope of the paper, we focus in Section 3 and 4 on the inverse models that have been developed for building damage and window breakage. These models are verified by their application to the Enschede firework disaster in 2000 [13, 14, 15] and the Khobar tower attack in 1996 [16, 17, 18, 19] respectively. The blast shielding effect in a densely built urban area is not taken into account in the relatively simple inverse models. This effect is illustrated with Computational Fluid Dynamics (CFD) simulations of the blast propagation in the Khobar tower geometry, and modelling of the window response with a Single Degree of Freedom (SDOF) model. In Section 5 conclusions are presented.

2. Combining multiple charge mass predictions

The post blast evidence leads to multiple charge mass predictions including an error estimate. The charge mass predictions can be of three types. In the first type, the observed damage can be translated to a prediction of the blast strength, which can be translated to a single value prediction of the charge mass when the distance from the explosion to the damaged object is known. However, many objects, e.g. windows, are either undamaged or completely broken. When such an object is broken, the result is a lower bound of the charge mass, while an undamaged object leads to an upper bound prediction. Practical considerations like the maximum load capacity of the vehicle used to carry the bomb may also lead to upper bounds. Single valued charge mass predictions are the most reliable type of data. Examples are façades where a part of the windows failed or where the building was damaged at an intermediate level.

A statistical method has been developed to combine the various types of data, in order to determine an overall charge mass distribution. For this purpose we have extended the least squares method for lower and upper bounds. The concept is that for lower bounds residuals are only taken into account for charge masses M below the boundary M_i, while for upper bounds residuals are only taken into account above the boundary. Although this concept seems quite obvious and straightforward, no description was found in literature. A more detailed description can be found in [22].

3. Building damage evidence

In this section we describe an existing model for the prediction of blast damage to brick buildings. Next we will derive the inverse form of the model and apply it to the Enschede firework disaster.

3.1 Model description

During World War II, damage from German bombings on England was analysed by E.B. Philip. She derived functions for the average damage radius for various levels of damage to typical U.K. houses (i.e. brick terraced dwellings). These were later declassified and published by Jarrett [8]. The original description gives only a short presentation of the building damage model. Stone and Henderson [5] give an extensive description of the model, its derivation and its background. Scilly and High [4] and Gilbert, Lees and Scilly [6] evaluated Philip's work and rewrote the equation into a form that uses the TNT-equivalent charge mass.

Gilbert, Lees and Scilly [6] published the following equation for the Average Circle Radius (ACR) as a function of the TNT equivalent charge mass (M):

$$ACR = \frac{RB \cdot k_{ACR} \cdot M^{\frac{1}{3}}}{\left[1 + \left(\frac{M_{ACR}}{M}\right)^2\right]^{\frac{1}{6}}} \qquad (1)$$

In this equation RB is the ratio of the ACR for a particular damage level to the ACR of damage level B. In Table 1 a description of the various damage levels is given, as well as the corresponding RB values. Eq. 1 contains the following constants: k_{ACR} = 7.1 m/kg$^{1/3}$, M_{ACR} = 3175 kg.

This work is mainly based on data from WW II air raids, so the criteria apply to the housing of that period: 1900 - 1940 style brick houses, single leaf wall, wooden floors and roof, 2 to 4 storeys high. It should be noted that the orientation of a building is not a variable in the model.

Table 1: Housing damage levels and RB ratio from Gilbert, Lees and Scilly [6].

Damage level	RB ratio	Description
A	0.675	Houses completely demolished, i.e. with over 75% of the external brickwork demolished
B	1.00	Houses so badly damaged that they are beyond repair and must be demolished when opportunity arises. Property is included in this category if 50% to 75% of the external brickwork is destroyed, or in the case of less severe destruction, the remaining walls have gaping cracks rendering them unsafe.
Cb	1.74	Houses which are rendered uninhabitable by serious damage, and need repairs so extensive that they must be postponed until after the war. Examples of damage resulting in such conditions include partial or total collapse of roof structures, partial demolition of one or two external walls up to 25% of the whole, and severe damage to load-bearing partitions necessitating demolition and replacement.
Ca	3.0	Houses that are rendered uninhabitable, but can be repaired reasonably quickly under wartime conditions, the damage sustained not exceeding minor structural damage, and partitions and joinery wrenched from fixings
D	6.0	Houses requiring repairs to remedy serious inconveniences, but remaining habitable. Houses in this category may have sustained damage to ceilings and tilings, battens and roof coverings, and minor fragmentation effects on walls and window glazing. Cases in which the only damage amounts to broken glass in less than 10% of the windows are not included.

3.2 Derivation of an inverse model

Building damage evidence consists of an observation of the damage level and the distance from the building to the explosion. For forensic analysis we are therefore interested in the inverse form of Eq. 1, expressing the TNT equivalent charge mass as a function of damage level and range. Mathematically the determination of the inverse form is quite straightforward. However, we should realize that in the inverse form some variables take on a different meaning and for clarity they are replaced by new variables. The ACR is replaced by the observed distance from the centre of the explosion to the centre of the building (r_{obs}). The ratio RB is replaced by RB_{obs}, the RB ratio for the observed damage level. This gives:

$$M = \frac{1}{2} \cdot \sqrt{2} \cdot \sqrt{\left(\frac{r_{obs}}{RB_{obs} \cdot k_{ACR}} \right)^3 \cdot \left[\left(\frac{r_{obs}}{RB_{obs} \cdot k_{ACR}} \right)^3 + \sqrt{\left(\frac{r_{obs}}{RB_{obs} \cdot k_{ACR}} \right)^6 + 4 \cdot M_{ACR}^2} \right]} \qquad (2)$$

In order to use this equation to determine a TNT equivalent charge mass including an error estimate, we have reanalysed the data from WW II. The original definition of the ACR of damage level B is: "a circle drawn around the centre of an explosion which damages dwelling houses such that there are as many damaged to the level of damage or greater outside the circle as there are of less than level B damaged inside the circle" [5]. This is illustrated in Figure 2 with one of the original bomb damage plots. The blue houses have damage level B, the yellow houses C. The inner circle is the ACR for damage level B. The number of blue houses outside this circle is equal to the number of yellow houses inside the circle.

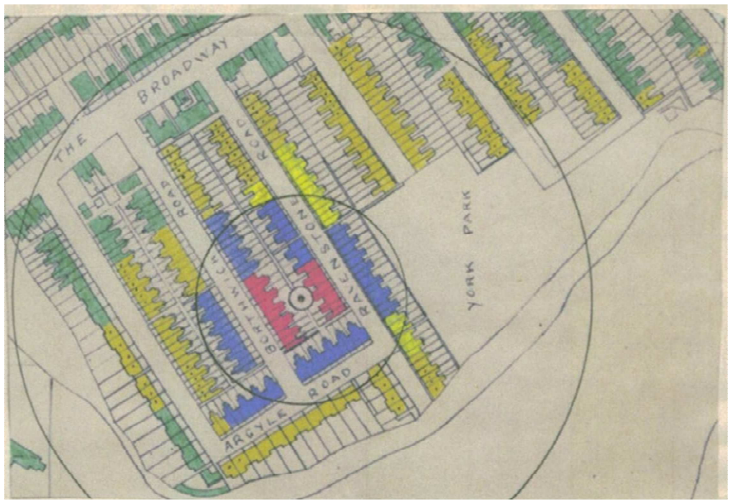

Figure.2: Typical bomb damage plot from Stone and Henderson [5] for a 2500 kg light alloy cased bomb in a moderately built up area. Damage level A (red), B (blue), C (yellow), and D (green).

From the data in the bomb damage plot cumulative distributions can be constructed for the various damage levels as in Figure 3. The figure shows that for the various damage levels the ACR does not correspond to the distance where 50% of the houses is damaged. The distributions could be reasonably well fitted with cumulative normal functions. It appeared that the mean of each distribution falls halfway between the ACRs for the relevant damage levels, e.g. the mean value of damage level B lies halfway between the ACR of damage levels A and B. Furthermore the coefficient of variation appeared to be about 30% for all damage levels. Available data on damage level C was not separated into Ca and Cb as in Table 1. The same logic as described above was followed to obtain results from Ca and Cb separately.

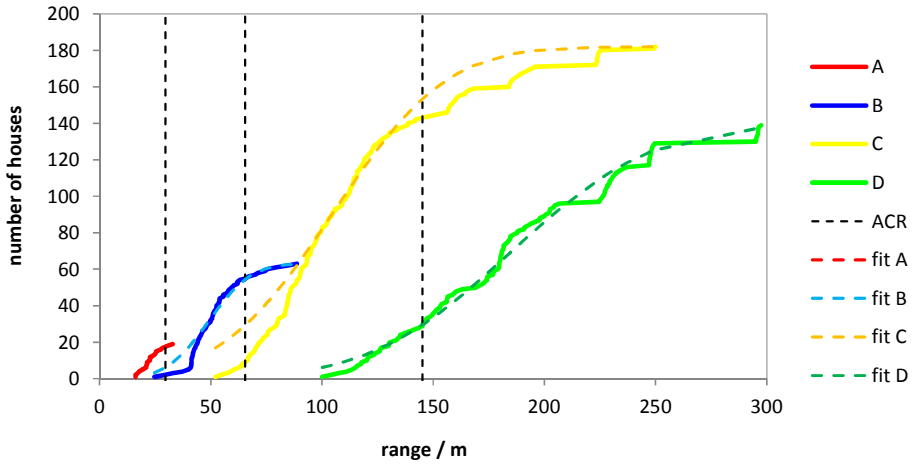

Figure. 3: Cumulative distribution for each damage category as a function of range together with datafits.

The original definition of damage level D has been extended to houses with less damage and undamaged houses. The reason is that in a forensic analysis the presence of the undamaged houses provides information as well, and is therefore desirable to include. Table 2 gives the resulting parameter values and also indicates whether the charge mass is a lower bound, single valued, or an upper bound.

Table 2: Values for the mean and standard deviation of RB_{ob}s for the various building damage levels. The result type of the charge mass is also indicated.

Damage level	RB_{obs} mean	RB_{obs} standard deviation	Result type (charge mass)
A	0.506	0.15	lower bound
B	0.838	0.25	single valued
Cb	1.37	0.41	single valued
Ca	2.37	0.71	single valued
C	2.00	0.6	single valued
D	4.5	1.35	upper bound

A mean TNT equivalent charge mass (μ) can now be determined by applying Eq. 2 with the appropriate mean value for RB_{obs} from Table 2. The standard deviation of the charge mass (σ) is determined using the standard deviation in RB_{obs} (σ_{RBobs}):

$$\sigma \cong \frac{M(RB_{obs}+\sigma_{RBobs}) - M(RB_{obs}-\sigma_{RBobs})}{2} \qquad (3)$$

3.3 Application to the Enschede firework disaster

In order to verify the inverse building damage model it has been applied to the Enschede fire work disaster.

A major fireworks accident occurred at S.E. Fireworks in Enschede in The Netherlands on the 13th of May 2000. Besides the destruction of a complete residential area, there were 21 deaths and 947 wounded. The events started with a relatively small explosion in a container, followed by an explosion in seven pre-fab storage facilities (so-called Mavo boxes). The final explosion in reinforced concrete storage cell C11 was the largest. Evidence collected by Weerheijm [13, 14, 15] consisted of data on building damage, window breakage, debris and the diameter of the fireball.

The current validation focusses on the third and largest explosion, and on the observed building damage only. The Enschede residential area consisted of brick walled dwellings that resemble the UK housing to a reasonable extent. The observed building damage is displayed in Figure 4.

Eq. 2 and 3 have been applied to a total of 184 building damage observations. The resulting charge mass predictions are plotted as function of range in Figure 5. Note that upper bound data are shown with a (semi-)infinite lower error bar, while the lower bound data are shown with a (semi-) infinite upper error bar. A striking feature is the saw tooth pattern which is caused by the discrete damage levels. Within each ‘tooth’ are buildings classified with the same damage level, but at various ranges.

When all data is combined using the procedure described in Section 2, we obtain a charge mass distribution with a mean charge mass of 3,461 kg, and a large coefficient of variation of 124 %. Charge masses between 1,315 kg and 9,107 kg are within one standard deviation from the average. These results are consistent with [16], where a range of charge masses from 2,330 to 7,050 kg was reported based on all damage categories. In this reference it was also concluded that a charge mass between 3,750 and 5,800 kg, based on damage category Cb only, is most realistic. This last interval is probably too narrow.

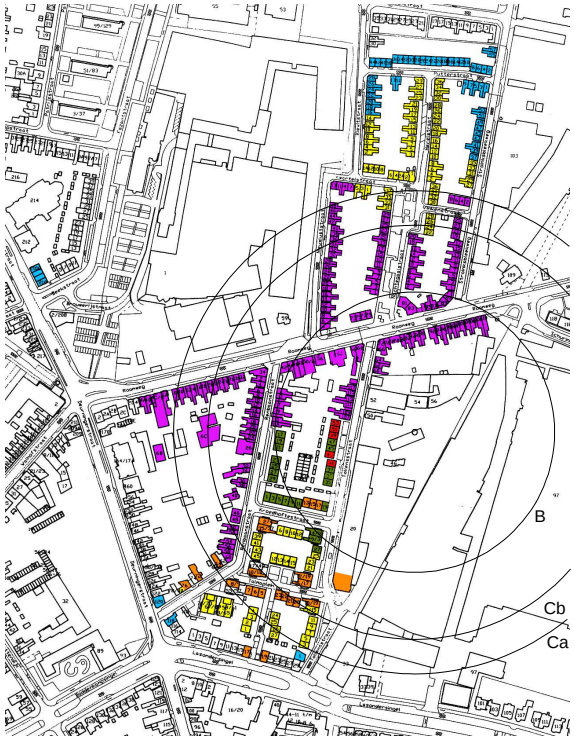

Figure. 4 Map of buildings that were damaged after the Enschede firework disaster. The buildings that are not coloured have very limited or no damage. Damage categories are indicated with colours: red (A), green (B), orange (Cb), yellow (Ca) and blue (D). Purple buildings are destroyed by fire and can therefore not be used as evidence.

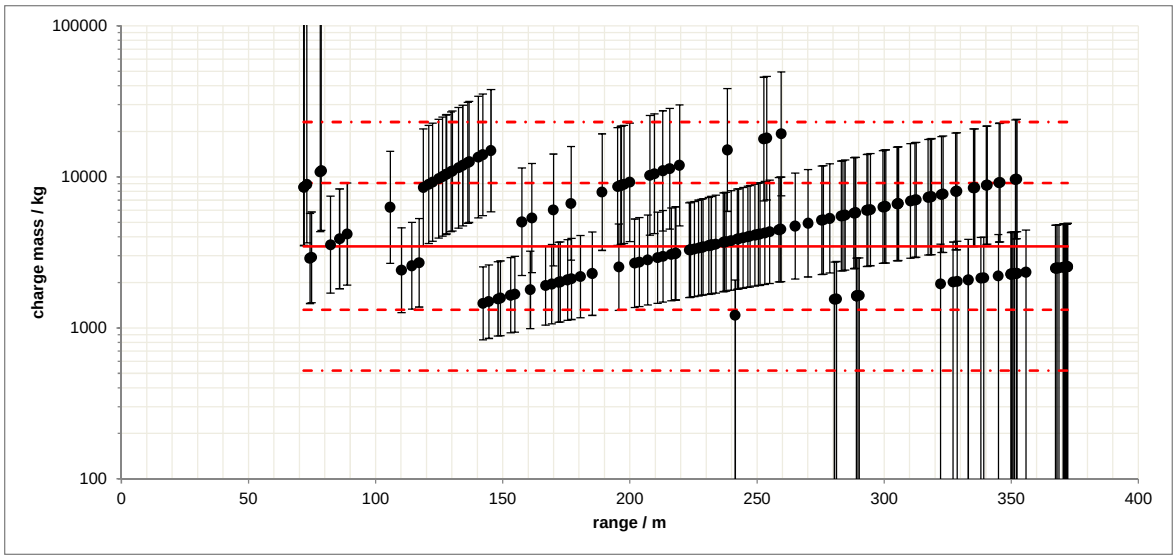

Figure. 5 Charge mass versus range. The red lines indicate the mean, plus and minus one standard deviation, and the 95% confidence limits.

4. Window breakage evidence

In this section we describe an existing model for the prediction of window breakage. Next we will derive the inverse form of the model and apply it to the Khobar tower attack.

4.1 Model description

A relatively simple existing model for the prediction of window breakage starts with an explosion on a surface, a so-called hemispherical surface burst. A blast wave can be characterized by its peak overpressure (P) and impulse (i); the area below the positive phase of the overpressure-time profile. While the blast wave propagates away from the explosion center, its peak overpressure and impulse decay with distance. A semi-empirical relation for the decay of the blast wave is given by Kingery and Bulmash [10, 21]. The blast wave will interact with infrastructure and load the façades of buildings. In the current simple model we distinguish between two extreme cases. Façades oriented parallel to the blast wave propagation direction will receive a side-on blast load. Façades facing the explosion will be loaded with a higher reflected blast load. Note that while the building damage model described in Section 3 did not explicitly take into account the orientation of a building, the model for window breakage does take this into account, since we are now considering specific façades.

The resistance of windows to a dynamic pressure load depends on the size and thickness of the window panes, and the type of glazing. This may vary from single or double annealed glazing to tempered, laminated or wired glass. TM5-1300 [9] provides a method to calculate the dynamic resistance in dependence of the window properties. The dynamic resistance is expressed in a so called P-i diagram; this is a curve that gives all combinations of the peak overpressure and impulse of a blast load that will result in the same breakage probability.

The above described model gives the probability of window breakage as a function of the TNT equivalent charge mass, range, façade orientation, and window properties. An overview is given in Figure 6.

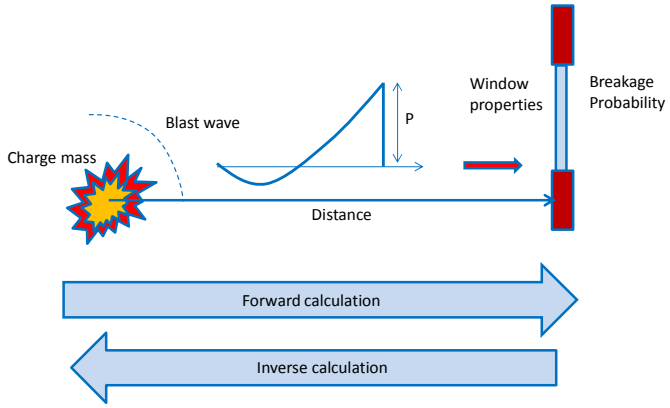

Figure. 6 Window breakage: forward and inverse calculation

4.2 Derivation of an inverse model

Window breakage evidence consists of an observation of the number of broken windows in a façade, the façade orientation, the window properties, and the range. It is important to verify whether windows were not already broken before the explosion took place, and whether windows failed due to the blast wave, and not due to other explosion effects (e.g. impacting debris and fragments).

For forensic analysis we are interested in an inverse form of the model described in Section 4.1. As a starting point we calculate a representative range of breakage probabilities for a façade. A more detailed description can be found in [22]. A minimum, mean and maximum breakage probability are now used to inversely calculate the charge mass and give an error estimate. In Section 4.1 it was mentioned that P-I curves are available for given window properties and breakage probability. These curves are shown schematically in Figure 7 for some example probabilities. The figure also shows

load curves for a fixed distance (in a forensic analysis the distance is known), and increasing charge mass. The intersections between the P-i curves and the load curves are resolved by an iterative calculation procedure and yield the desired range of charge masses.

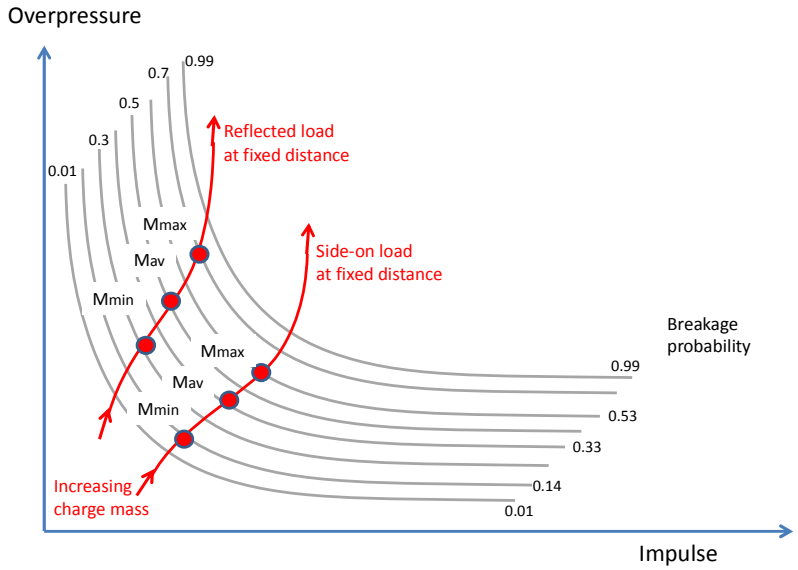

Figure. 7 Schematic P-I curves for glazing together with load curves for a fixed distance and varying charge mass. Probabilities have been selected for the two cases outlined in Figure 10, and based on Figure 12.

4.3 Application to the Khobar tower attack

On June 25, 1996, a terrorist's truck bomb exploded at the Khobar Towers housing compound in Dhahran, Saudi Arabia, killing 19 American service personnel and wounding 555 [16, 17, 18, 19]. The force of the explosion was so great it heavily damaged and destroyed high rise apartment buildings, shattered numerous windows and left a massive crater in the ground.

Figure. 8 Overview of the Khobar Towers compound in Dhahran Saudi Arabia, 1996

The current validation considers window breakage only. The windows involved were two fixed glass façade panels and one sliding door (also called patio door) for each apartment. Window properties were not available, but have been estimated based on publicly available pictures to be single annealed 6 mm glazing with dimensions of 2.05 by 0.83 m. The observed window breakage at the Khobar tower compound is displayed in Figure 9. The various façades contained either 24 or 12 windows.

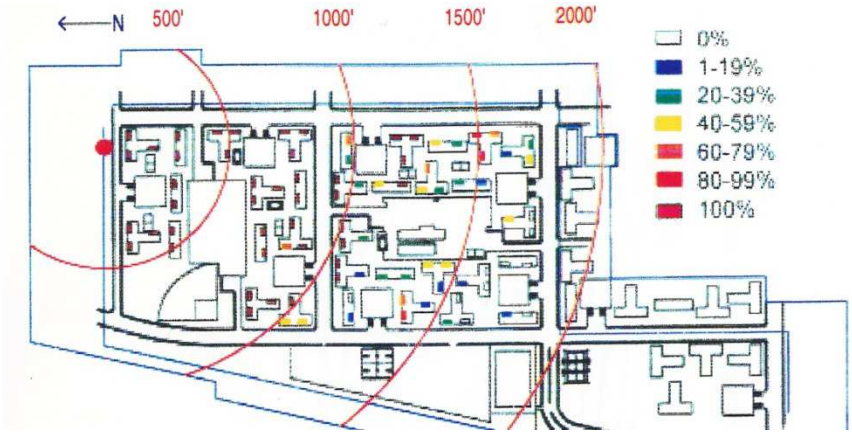

Figure. 9 Patio door glass breakage at the Khobar tower compound [19]

The inverse model presented in Section 4.2 has been applied to a total of 57 sets of windows. The resulting charge mass predictions are plotted as function of range in Figure 10. Note that upper bound data are shown with a (semi-)infinite lower error bar, while the lower bound data are shown with a (semi-) infinite upper error bar.

When all data is combined using the procedure described in Section 2, a charge mass distribution with a mean of 5,658 kg, and a coefficient of variation of 70 % is obtained. Charge masses between 3,019 kg and 10,602 kg are within one standard deviation from the average. This range of charge masses is significantly smaller than published by DSWA [18]. They reported a charge mass of 30,000 lbs or 13,600 kg based on window breakage.

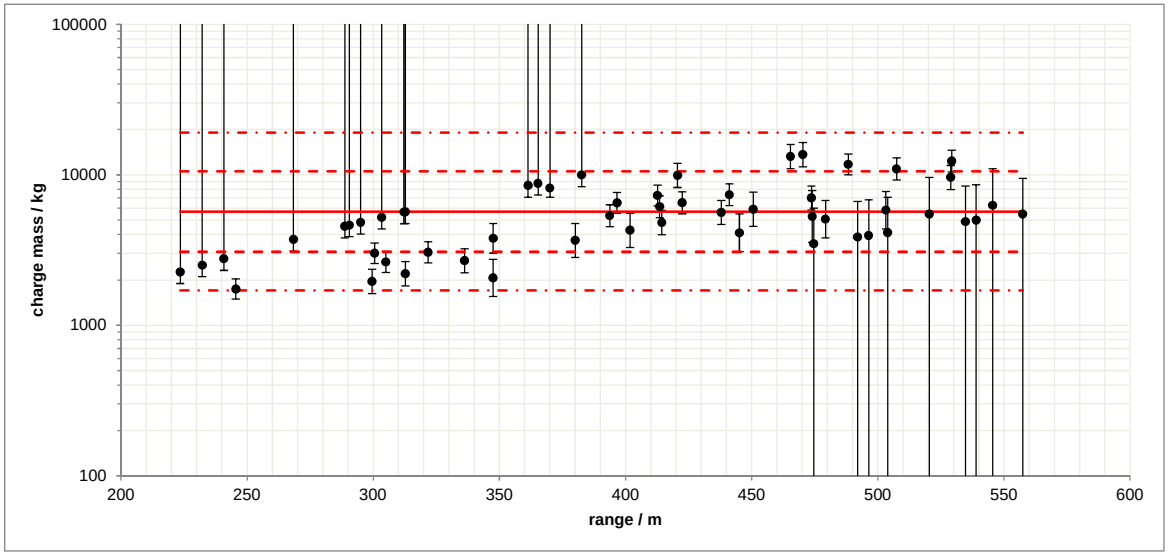

Figure. 10 Charge mass versus range. The red lines indicate the mean, standard deviation limits, and the 95% confidence limits.

4.4 Detailed analysis of the Khobar tower attack

The observed difference in Section 4.3 may be caused by the fact that DSWA based their findings on a detailed (not publicly available) analysis taking into account blast shielding effects. These effects are not addressed in the developed inverse model. In order to investigate this hypothesis the blast propagation through the Khobar tower geometry was simulated with Autodyn [20].

In this section two simulations are presented; one with a charge mass of 5,436 kg (as predicted by the inverse model), and 13,600 kg (as published by DSWA). In both simulations overpressure profiles have been recorded on various building façades. These profiles constitute inputs to a Single Degree of Freedom (SDOF) model to determine the window response and breakage probability. The breakage probability is then compared to the observed damage to assess the plausibility of the assumed charge mass.

The simulation setup is displayed in Figure 11 showing the bomb location, the layout of the buildings and the location of the pressure gauges. One gauge is assigned per apartment. Note that the building closest to the bomb location is omitted from the simulation due to numerical difficulties. As a result the pressure load on the other buildings is slightly overestimated.

Initialization of the simulation is performed in a one-dimensional (1D) grid using spherical coordinates. This simulation is stopped slightly before the blast reaches the first building which is approximately 80 m from the bomb location. A cell size of 2 mm is used for the 1D simulation to accurately resolve the blast profile. The flow field is then mapped from the 1D simulation into a 3D numerical domain as shown in Figure 12. The cell size of the numerical domain is approximately 1.2 m for a total of approximately 28 million cells (the domain size is 550 x 400 x 225 m).

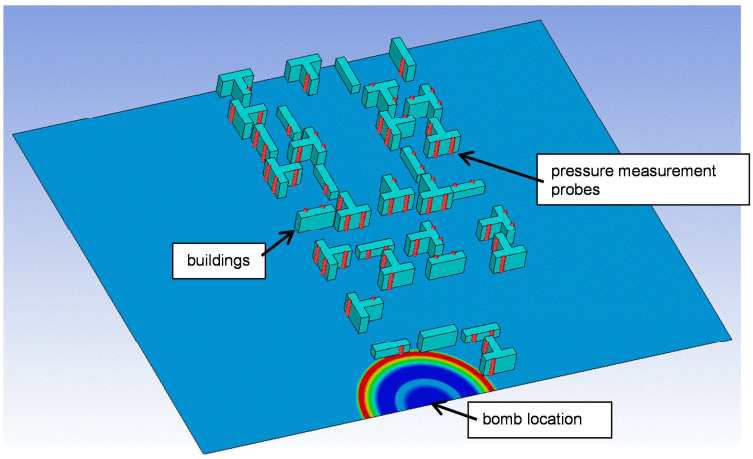

Figure. 11 Simulation setup showing the bomb (bottom), buildings and pressure measurement probe locations (red).

The pressure contours for the 13,600 kg simulation are presented in Figure 12 at two instances showing the effect of the buildings on the shock front and on the flow pattern behind it.

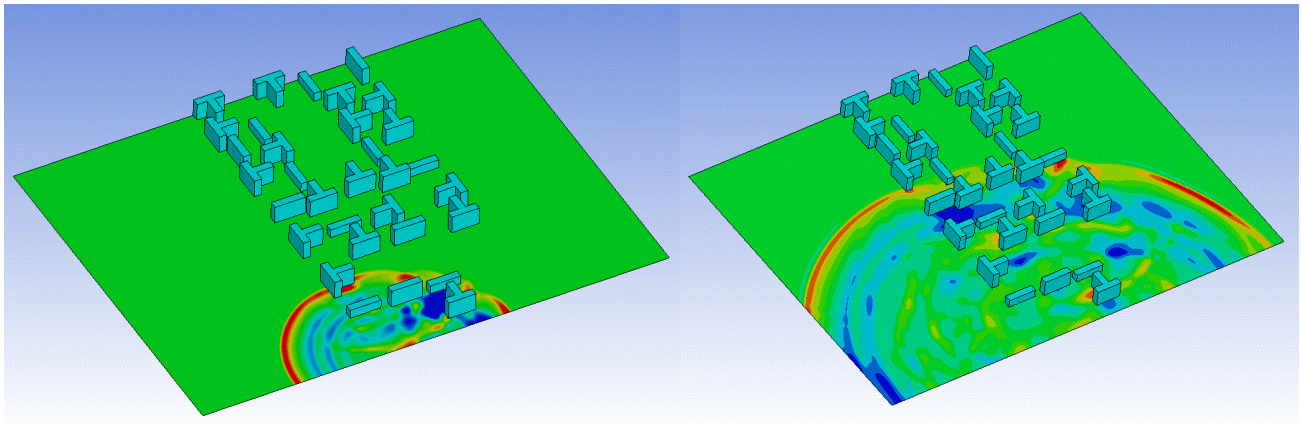

Figure. 12 Overpressure contours for the 13,600 kg simulation at 220 ms (top) and 820 ms (bottom).

For each façade an average probability of window breakage has been calculated. Figure 14 presents the results for the 5,436 kg and 13,600 kg simulations, as well as the observed probability of window breakage.

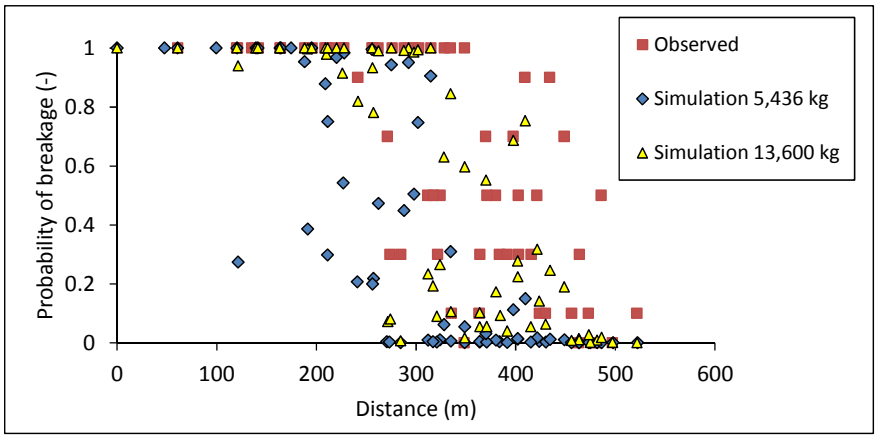

Figure. 14 Comparison between the observed breakage probability and the simulations for 5,436 kg and 13,600 kg

As expected the 13,600 kg simulation consistently shows higher probabilities compared to the 5,436 kg simulation. The 13,600 kg simulation shows a much better agreement with the observed breakage probability. A striking feature is that the scatter in the observations is significantly larger than in the simulations. Further variation of the charge mass or the inclusion of the building closest to the bomb location, could lead to an even better charge mass prediction (i.e. with a smaller difference with the observed breakage probabilities). This has however not been conducted in the current study.

5. Conclusions

The Inverse Explosion Analysis (IEA) tool was developed to estimate the TNT equivalent charge mass and point of origin based on observed damage around an explosion. A statistical method has been developed to combine various types of data, and to determine an overall charge mass distribution. In this paper inverse models have been presented for the two most frequently occurring and reliable sources of information: window breakage and building damage. The models have been verified by applying them to the Enschede firework disaster and the Khobar tower attack.

Close-in to the explosion, buildings with the highest damage level and façades of which all windows are broken lead to lower bound charge mass predictions. In the far field undamaged buildings and façades without window breakage lead to upper bound predictions. The most valuable data comes from the intermediate region.

In relatively open environments, like for the Enschede firework disaster, the models generate realistic charge masses that are consistent with values found in forensic literature. The confidence interval predicted by the IEA tool is however mostly larger than presented in the literature. This is realistic due to the large inherent uncertainties. To our judgment often a too narrow range of charge masses is presented, compared to the evidence. The IEA models give a reasonable first order estimate of the charge mass in a densely built urban environment, such as for the Khobar tower attack. Due to blast shielding effects which are not taken into account in the IEA tool, this is usually an under prediction. To obtain more accurate predictions, the application of Computational Fluid Dynamics (CFD) simulations is advised.

The TNO IEA tool gives unique possibilities to inversely calculate the TNT equivalent charge mass based on a large variety of explosion effects and observations. The IEA tool enables forensic analysts, also those who are not deep experts on explosion effects, to perform an analysis with a largely reduced effort.

Acknowledgments

The research leading to these results has received funding from the European Community's Seventh Framework Programme (FP7/2007 - 2013) under grant agreement n° 284585.

References

[1] Thurman, James T., *Practical Bomb Scene Investigation*, Second Edition, 2011 T&F Group, LLC

[2] Beveridge, A., *Forensic Investigation of Explosions*, Second Edition, 2012, CRC Press, T&F Group.

[3] National Institute of Justice, US Department of Justice, *A guide for explosion and bombing scene investigation*, Research Report. https://www.ncjrs.gov/pdffiles1/nij/181869.pdf

[4] Scilly, N.F. and High, W.G., *The Blast Effects of Explosions*, 85th Int. Symp. Loss Prevention in the Process Industries, Cannes 15-19 September 1986, vol. 1, paper 39.

[5] Stone, P.D., Henderson, J., *World War II bomb damage, accidental explosions and the basis of our current quantity distances*, 32nd Explosives Safety Seminar, 2006.

[6] Gilbert, S.M., Lees, F.P., Scilly, N.F., *A model for hazard assessment of the explosion of an explosives vehicle in a built-up area*, 26th DoD Explosives Safety Seminar, Miami, 1994 (pap12c1.pdf).

[7] Glasstone, S., Dolan, Ph.J., *The effects of nuclear weapons*, US Dept. of Defense, Washington, 1977.

[8] Jarrett, D.E., *Derivation of the British explosives safety distances*, Annals of the New York Academy of Sciences, vol. 152 (1968).

[9] TM 5-1300, *Structures to resist the effects of accidental explosions*, Departments of the Army, the Navy, and the Air Force, TM 5-1300, NAVFAC P-397, AFR 88-22, Washington, D.C., November 1990. superseded by: UFC 3-340-02 Structures to Resist the Effects of Accidental Explosions, 2008.

[10] Kingery, C.N.; Bulmash, G., *Airblast parameters from TNT spherical air burst and hemispherical surface burst*, Ballistic Research Laboratory, Technical Report ARBRL-TR-02555, Aberdeen, MD, April 1984.

[11] Agresti, Alan; Coull, Brent A. (1998*). "Approximate is better than 'exact' for interval estimation of binomial proportions."* The American Statistician 52: 119–126.

[12] Christensen, S.O., Hjort, Ø.J.S., *Back Calculation of the Oslo Bombing on July 22nd, using window breakage*, NDEA, MABS symposium 2012.

[13] Weerheijm, J., Van Wees, R.M.M, de Bruyn, P.C.A.M., Karelse, J.W., *The Fireworks Disaster in Enschede, Part 1: Overview and Reconstruction*, DoD Explosives Safety Seminar 2002

[14] Weerheijm, J., Van Wees, R.M.M., de Bruyn, P.C.A.M., Karelse, J.W., *The Fireworks Disaster in Enschede, Part 2: Safety & Pyrotechnics*, ISEM2002, Japan

[15] Weerheijm, J., Van Wees, R.M.M., Van Doormaal, J.C.A.M. Rhijnsburger, M.P.M., *De explosies bij S.E. Fireworks. Deel 1: de kracht van de explosies op basis van waargenomen schade*. PML 2000-C120. Januari 2000.

[16] Spence, F.D., *The Khobar Towers Bombing Incident*, Staff Report National Security Committee House, August 14, 1996

[17] Thompson, D., Brown, S., Mallonee, S. and Sunshine, D., *Fatal and non-fatal injuries among U.S. Air Force personnel resulting from the terrorist bombimg of the Khobar Towers*, The journal of Trauma Injury, Infection, and Critical Care,Vol. 57, No. 2, August 2004, pp. 208-215

[18] Special Weapon Agency (DSWA), *Report of Khobar Towers Bomb Damage Survey*, July 1996

[19] Jamieson, P.D., *Khobar Towers, Tragedy and Response*, Air Force History and Museums Program, United States Air Force, Washington, D.C. 2008

[20] Hayhurst, C.J., Clegg, R.A. and Cowler M.S., *New Models and Hydrocodes for Shock Wave Processes in Condensed Matter*, Edinburgh, 2002.

[21] AASTP-4, *Allied Ammunition Storage and Transport Publication, Manual on Explosives Safety Risk Analysis*, Edition 1, Change 2, NATO International Staff, Defence Investment Division, November 2008

[22] van der Voort, M.M., van Wees, R.M.M., Brouwer, S.D., van der Jagt-Deutekom, M.J., Verreault, J., *Forensic analysis of explosions: inverse calculation of the charge mass*, Volume 252, July 2015, Pages 11–21. doi:10.1016/j.forsciint.2015.04.014.

[23] van der Voort, M.M., van Wees, R.M.M., Brouwer, S.D., van der Jagt-Deutekom, M.J., Verreault, J., A structured approach to forensic study of explosions: The TNO Inverse Explosion Analysis tool, 5th DAPS conference, 19-21 May 2015, Singapore.